Astron. Astrophys. 361, 19–32 (2000)

ASTRONOMY AND ASTROPHYSICS

H I observations of emission-line galaxies

J.V. Smoker[1,2], R.D. Davies[2], D.J. Axon[3], and E. Hummel[2]

[1] Astrophysics and Planetary Science Division, Department of Pure and Applied Physics, The Queen's University of Belfast, University Road, Belfast, BT7 1NN, UK
[2] University of Manchester, Jodrell Bank Observatory, Macclesfield, Cheshire, SK11 9DL, UK
[3] Department of Physical Sciences, University of Hertfordshire, College Lane, Hatfield, AL10 9AB, UK

Received 3 April 2000 / Accepted 6 July 2000

Abstract. We present single-dish Lovell telescope H I observations of a sample of 67 emission-line and UV-excess galaxies, of which 52 are taken from the University of Michigan (UM) catalogue. In addition, H I observations of 24 gas-rich irregular galaxies are presented. We find that emission-line galaxies are H I–rich with a median H I mass to blue luminosity ratio M_{HI}/L_B of ~ 0.45 $M_\odot/L_\odot$. Within the UM galaxy sample the M_{HI}/L_B ratio tends to increase with decreasing luminosity. Finally, it is found that the most H I–rich UM galaxies are the most metal deficient, implying that these objects are less evolved.

Key words: galaxies: compact – galaxies: fundamental parameters – galaxies: irregular – radio lines: galaxies

1. Introduction

Emission-line galaxies (EmLGs), or extragalactic H II regions as they are also known, are galaxies with a blue stellar continuum dominated by O and B stars and high emission-line equivalent widths, indicative that stars have recently been formed. Observed Hβ luminosities are generally in the range 10^{40} to 10^{41} erg s^{-1} with some objects reaching 10^{43} erg s^{-1} (Salzer et al. 1989b; Terlevich et al. 1991). Their spectroscopic properties are indistinguishable from those of giant H II regions and they are thus frequently referred to as H II galaxies. The University of Michigan survey used the [OIII] $\lambda\lambda$4959,5007 and [OII] $\lambda\lambda$3726,3729 doublets to discover hundreds of such EmLGs. The current paper describes H I observations of a sample of UM galaxies and compares them with previous studies of UV-excess galaxies.

Emission-line galaxies have a range of morphologies and span a wide range in absolute magnitude, from galaxies with $M_B \approx$ –23 to dwarf 'Sargent-Searle' objects with $M_B \approx$ –14. Often it is found that the galaxies are either interacting or disrupted, although many are more primitive systems with no obvious spiral structure. The smaller objects in this class are often referred to as blue compact galaxies (BCGs), although these galaxies are generally selected on the basis of a blue colour, UV-excess or compactness rather than emission-line strength. Examples of BCGs are objects found in the Haro, Markarian or Zwicky galaxy catalogues (Haro 1956; Markarian 1967; Markarian et al. 1981; Zwicky 1971). UV-excess selected galaxies such as the Markarian sample show a range in spectral properties; from galaxies with absorption-line spectra to narrow emission-line objects classified as H II galaxies (Huchra 1977; Khachikian 1987). Approximately 40% of Markarian galaxies with absolute magnitudes in the range from –17.5 to –22.5 display starburst type spectra (Balzano 1983), with perhaps as many as 70% of all Markarian objects having narrow emission-line spectra similar to H II regions (French 1980). Hence a substantial proportion of galaxies selected by UV-excess and emission-line strength criteria are the same type of object, with many galaxies being present in both the Markarian (UV-excess) and University of Michigan (EmLG) catalogues. However, the two populations taken as a whole show differences. For example, the width of the $(B-R)$ colour distribution of the EmL UM galaxies is greater than that of the UV-excess Markarian galaxies (Salzer et al. 1989a) although their mean values are similar.

Previous neutral hydrogen studies of UV-excess and blue compact galaxies have been undertaken by Gordon & Gottesman (1981), Thuan & Martin (1981) and Staveley–Smith et al. (1992). These latter studies have focussed on the Haro, Markarian, and Zwicky lists of galaxies and hence were selected on the basis of a strong UV–continuum or compactness and not on emission-line strength. Accordingly, one of the aims of the present survey was to determine whether the H I properties, for example the fractional H I contents, of the true emission-line galaxies are similar to the UV-excess selected objects. This study compliments that of Thuan et al. (1999), who also studied the H I properties of a sample of objective-prism-selected objects taken from the first and second Byurakan surveys (Markarian et al. 1983,1989).

2. Observations

2.1. The sample

The present sample of emission-line galaxies observed in H I includes a total of 52 galaxies taken from the UM catalogues. Of these, 32 objects are from the University of Michi-

Send offprint requests to: J.V. Smoker (j.smoker@qub.ac.uk)

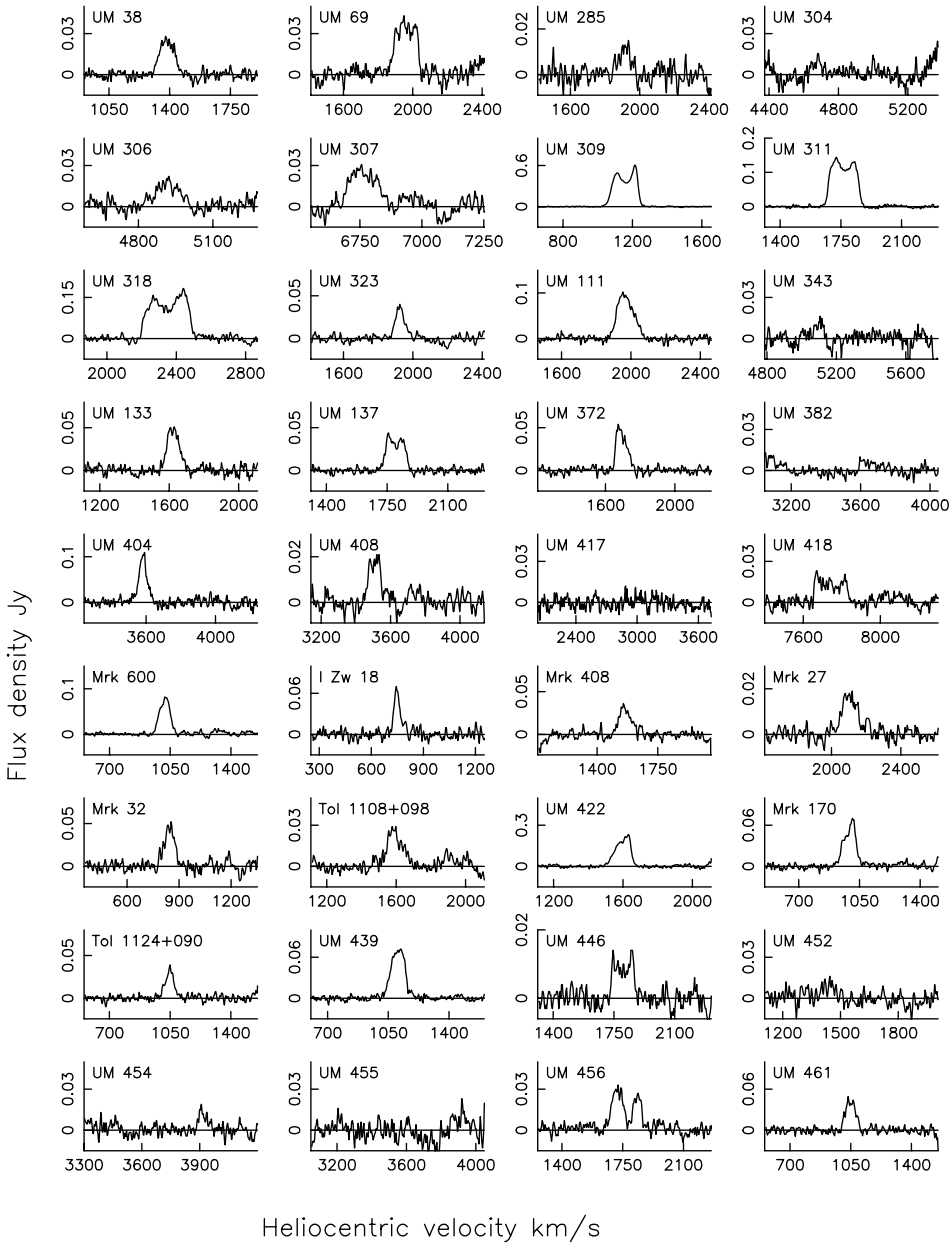

Fig. 1. H I spectra of the emission-line and blue compact galaxies. The flux scale is uncorrected for beam dilution. Heliocentric velocity is in the optical convention, v=c$\Delta\lambda/\lambda_0$.

gan sample lists IV and V with heliocentric velocities of less than 3000 km s^{-1} (MacAlpine & Lewis 1978; MacAlpine & Williams 1981) and 13 galaxies with $V_{\rm Hel} > 3000$ km s^{-1}. CCD imaging and spectroscopy of these galaxies has previously been undertaken by Salzer et al. (1989a,b), with coadded IRAS fluxes being presented in Salzer & MacAlpine (1988). Seven further EmLGs from other UM lists and two 'Tololo' emission-line galaxies from Bohuski et al. (1978) were also included. The present paper is complimentary to H I synthesis observations of over 20 EmLGs by Taylor et al. (1993, 1995), most of whose targets are in common with this paper.

A comparison sample of 13 blue compact and UV-excess galaxies were also observed in H I. These objects largely originate from the Markarian sample of galaxies (n=10), with a single object also included from the Zwicky catalogue. Observations of these galaxies allow an internal comparison to be made with the true emission-line galaxies taken from the University of Michigan survey.

Finally, in order to obtain good H I spectra for future H I mapping of a sample of irregular galaxies, we observed 24 irregular galaxies with high M_{HI}/L_B ratios which are presented separately from the emission-line galaxies. These data have a superior signal-to-noise ratio compared with existing spectra.

2.2. H I observations

The H I observations of the galaxies in this sample were taken in sessions between 1990 and 1994 with the 76-m Lovell Telescope at Jodrell Bank. The autocorrelation spectrometer (Pointon 1977) was used to integrate the data and was split

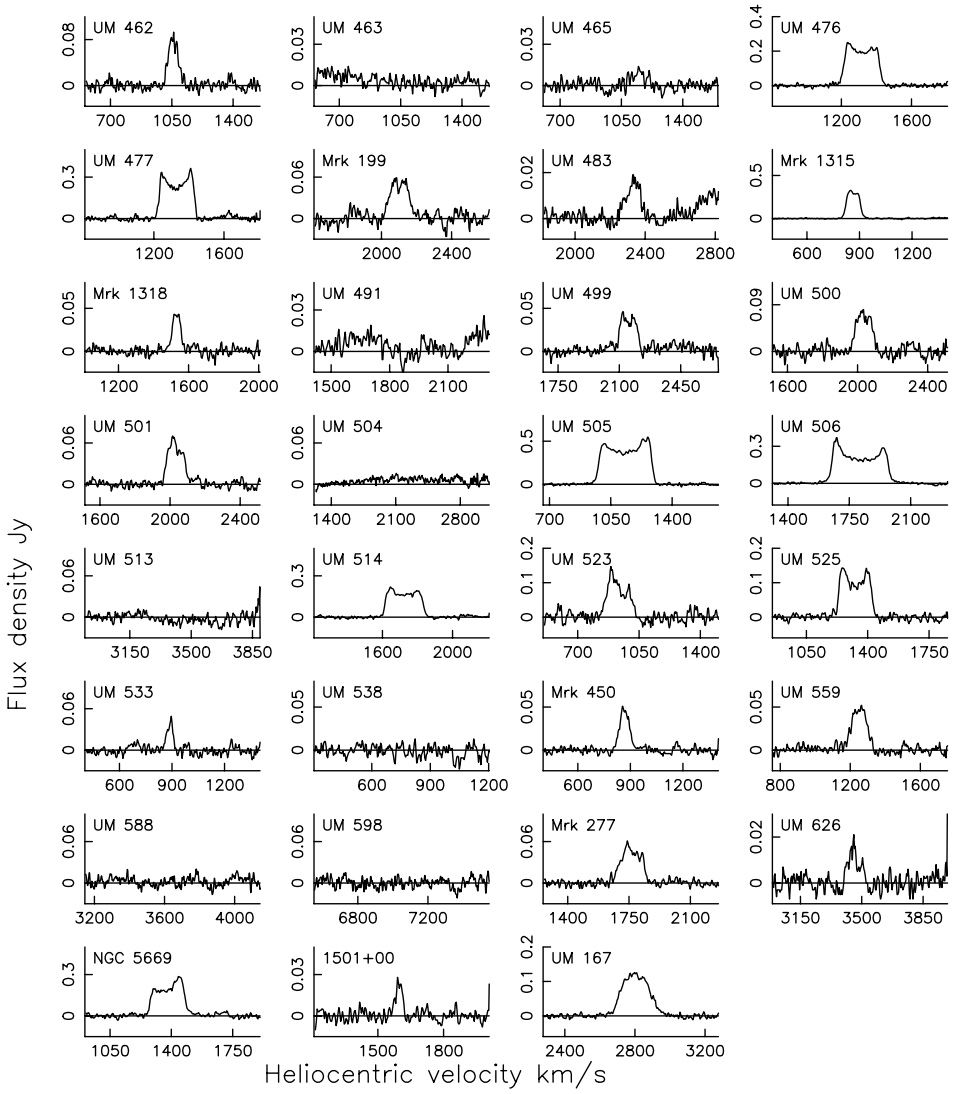

Fig. 1. (continued)

into two 512 channel banks for the right and left circular polarizations. The bandwidth used in each polarization was 5 or 10 MHz with the resulting velocity resolution of the final spectra being 3.7 and 7.4 km s^{-1} respectively. Data were calibrated using the H I-line calibrators NGC 1058 and NGC 4214 which were assumed to have flux density integrals of 74.9 Jy km s^{-1} and 191.0 Jy km s^{-1}, respectively, before correction for beam filling (Staveley-Smith 1985). Typical integration times were 1 hour for the large galaxies and 12 hours for the faint objects with typical final rms noise values being 4 mJy per channel.

Standard reduction procedures were used to obtain the final spectra displayed in Fig. 1 (EmLGs and BCGs) and Fig. 2 (gas rich irregulars). This data reduction involved removing interference spikes, fitting of 3rd–4th order polynomials to the individual spectra to remove baseline curvature, and calibration of the two polarizations separately. The calibrated spectra were added and a weighted average formed from the two polarizations. Of the 67 emission-line and blue compact galaxies observed in H I, a total of 53 were detected at a level greater than 3σ per channel. All 24 of the gas–rich irregulars were detected in H I. Errors in the flux density integral and velocity parameters were estimated by comparing the derived values for the two channels. Comparison with Fisher & Tully (1975,1981a) (n=23) indicates that our flux density scale is higher by $\sim 5\%$ with total errors in the flux density integral generally being less than 10%. Errors in the derived heliocentric velocities and velocity widths are of order 5 km s^{-1} to 20 km s^{-1}, depending upon the signal strength.

2.3. Observed properties

The observational data for the final galaxy sample are listed in Table 1 for the emission-line and blue compact galaxies and in Table 2 for the gas–rich irregulars. The column entries for the tables are as follows;

(1) Galaxy identification. TOL, Tololo galaxy (Bohuski et al. 1978); Mrk, Markarian catalogue of galaxies (Markarian 1967; Markarian et al. 1981); NGC, New General Catalogue and IC, Index Catalogue (Dreyer 1888,1895); UGC, Uppsala General Catalogue (Nilson 1973); UM, University of Michigan cat-

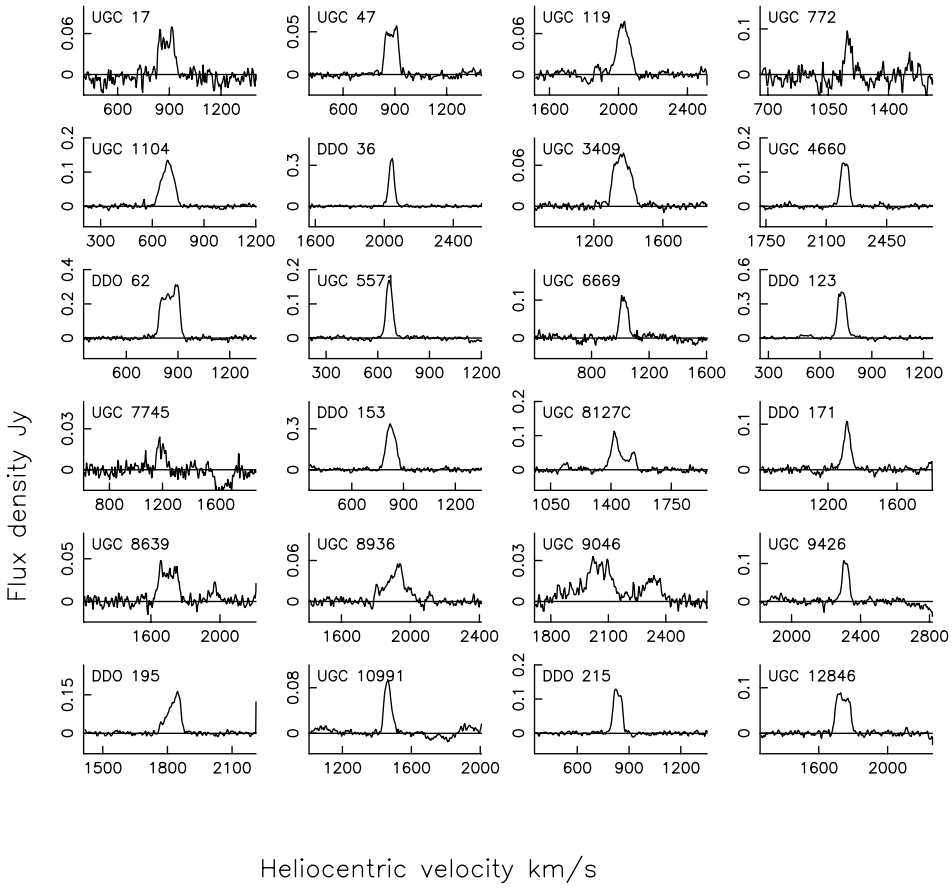

Fig. 2. H I spectra of the gas–rich irregular galaxies. The flux scale is uncorrected for beam dilution. Heliocentric velocity is in the optical convention, v=c$\Delta\lambda/\lambda_0$.

alogue (MacAlpine & Lewis 1978; MacAlpine & Williams 1981); Zw, Zwicky catalogue (Zwicky 1971).
(2) Alternative identification.
(3) Galaxy type.
(4) Right ascension and declination in B1950 coordinates observed with the Lovell Telescope.
(5) *Line 1:* Linear diameter in arcmin, D'_{25}. This is the diameter at a surface brightness limit of μ_B=25 mag arcsec^{-2} which corresponds to the value given in the Second and Third Reference Catalogues of galaxies (RC2, RC3; de Vaucouleurs et al. 1976; de Vaucouleurs et al. 1991). In the cases where a D'_{25} diameter was not available from the literature, one was measured directly from the 'O' prints of the Palomar Sky Survey and converted to D'_{25} using the precepts in the RC2.

Line 2: Axial ratio at the D'_{25} diameter, r_{25}.

(6) *Line 1:* Heliocentric velocity in km s^{-1}, $V_{\rm Hel}$, corrected to the optical convention v=$c\Delta\lambda/\lambda_0$. This is the velocity mid-way between the half power points measured at each side of the spectrum. Gaussian fitting to each side of the spectra was also used to determine the half power points. These latter values are shown in brackets. Where no H I was detected in the UM sample we give the optical redshift taken from Salzer et al. (1989a).

Line 2: Error in $V_{\rm Hel}$ in km s^{-1}.

(7) *Line 1:* Velocity width in km s^{-1}, W_{50}, being the directly-measured full width half maximum velocity width. The corresponding FWHM value obtained using gaussian fitting to the profile edges is shown in brackets.

Line 2: Error in W_{50} in km s^{-1}.

(8) *Line 1:* Flux density integral in Jy km s^{-1}, FI, not corrected for beam dilution.

Line 2: Error in FI in Jy km s^{-1}.

(9) RMS noise value per channel in mJy, $\sigma_{\rm RMS}$.
(10) Apparent blue magnitude, $B_{\rm T}$.
(11) *Line 1:* Source of the magnitude data. Where possible we have tried to use CCD magnitudes or data from RC3.

Line 2: Source of diameter data. The following abbreviations have been used for either $B_{\rm T}$ or D'_{25};

CMM93, Campos-Aguilar et al. (1993); DCC99, Doublier et al. (1999); DDB83, de Vaucouleurs et al. (1983); GPPMR96, Garnier et al. (1996); ISIB96, Impey et al. (1996); KKR99, Karachentseva et al. (1999); RC3, de Vaucouleurs et al. (1991); SAD99, Smoker et al. (1999); SDAH00, This paper; SDK92, Staveley–Smith et al. (1992); TBGS95, Taylor et al. (1995); TM81, Thuan & Martin (1981); UGC, Nilson (1973).

For RC3 magnitudes m_B refers to a photographic magnitude and $B_{\rm T}$ to a photoelectrically-calibrated or photoelectric magnitude.

Table 1. Observational data for the emission-line and blue compact galaxy sample.

(1) Galaxy	(2) Alternative name(s)	(3) Type	(4) R.A. Dec. (B1950)	(5) D'_{25} r_{25}	(6) $V_{\rm Hel}$ σ km s^{-1}	(7) W_{50} σ km s^{-1}	(8) FI σ Jy km s^{-1}	(9) $\sigma_{\rm RMS}$ channel^{-1} mJy	(10) B_T mag.	(11) Mag. ref. Diam. ref.
UM 38		EmL	00 25 18	0.63	1380 (1381)	104 (100)	2.6	2.7	15.50	GPPMR96
			03 13 00	0.76	16	16	0.4			GPPMR96
UM 69	IC 52, UGC 494	EmL	00 45 48	0.95	1952 (1955)	143 (144)	5.2	4.0	15.17	m_B(RC3)
			03 49 00	0.43	14	14	0.7			RC3
UM 285		EmL	00 49 26	0.31	1908 (1913)	123 (78)	0.9	3.4	17.33	SDK92
			–01 56 36	0.55	30	30	0.5			SDK92
UM 304		EmL	01 04 18	0.69	4730?	–	–	4.6	15.40	ISIB96
			01 40 42	0.62						SDAH00
UM 306		EmL	01 07 59	0.49	4914 (4916)	145 (120)	2.5	4.0	16.20	CMM93
			01 50 56	0.48	20	20	0.6			SDAH00
UM 307	UGC 749, ARK 33	EmL	01 08 56	1.00	6762 (6764)	137 (134)	3.3	3.6	14.31	m_B(RC3)
			01 03 24	0.34	8	8	0.6			RC3
UM 309	NGC 428, UGC 763	EmL	01 10 22	3.67	1152 (1150)	158 (158)	74.0	4.2	11.90	SAD99
			00 43 01	0.74	2	2	4.0			SAD99
UM 311	NGC 450, UGC 807	EmL	01 13 00	3.33	1760 (1762)	178 (176)	21.7	3.2	12.64	SAD99
			–01 06 00	0.66	2	2	1.5			SAD99
UM 318	NGC 493, UGC 914	EmL	01 19 33	3.39	2350 (2343)	273 (263)	36.2	9.0	12.93	B_T(RC3)
			00 41 13	0.31	6	6	3.0			RC3
UM 323		EmL	01 24 12	0.46	1923 (1920)	55 (58)	2.4	4.0	15.95	CMM93
			–00 54 15	0.75	18	18	0.5			SDAH00
UM 111	UGC 1102 Galaxy Pair	EmL	01 29 52	1.10	1966 (1964)	117 (110)	10.8	5.9	13.88	GPPMR96
			04 20 48	1.00	12	12	1.0			GPPMR96
UM 343	NGC 622, UGC 1143, MRK 571	EmL	01 33 25	1.82	5161	–	–	3.2	13.71	B_T(RC3)
			00 24 29	0.71						RC3
UM 133		EmL	01 42 08	0.93	1620 (1620)	77 (81)	4.2	4.5	15.38	m_B(RC3)
			04 38 48	0.27	18	18	0.6			RC3
UM 137	UGC 1240	EmL	01 43 48	1.15	1792 (1798)	125 (125)	4.5	3.0	14.75	m_B(RC3)
			04 01 12	0.36	8	8	0.6			RC3
UM 372	UGC 1297	EmL	01 47 35	1.05	1689 (1686)	85 (82)	3.6	3.3	14.81	m_B(RC3)
			02 03 38	0.78	8	8	0.4			RC3
UM 382		EmL	01 55 35	0.24	3598	–	–	3.0	18.56	CMM93
			–00 21 12	0.90						SDAH00
UM 404	1.0′ from CGCG 387–050	EmL	02 07 39	1.46	3580 (3581)	47 (47)	6.2	6.5	18.40	CMM93
			–01 38 57	0.37			0.6			SDAH00
UM 408		EmL	02 08 48	0.26	3507 (3506)	77 (77)	1.5	3.2	17.58	CMM93
			02 06 26	0.68	8	8	0.4			SDAH00
UM 417		EmL	02 16 55	0.27	2698	–	–	4.0	18.20	DCC99
			–01 12 57	0.57						DCC99
UM 418	UGC 1794, MRK 592	EmL	02 17 07	1.15	7736 (7737)	175 (175)	2.5	2.9	14.30	m_B(RC3)
			–00 29 06	0.81	8	8	0.5			RC3
MRK 600		UvES	02 48 30	0.56	1014 (1011)	72 (71)	5.8	3.5	15.42	DCC99
			04 15 00	0.54	8	8	0.5			DCC99
I Zw18	UGCA 166, MRK 116	UvES	09 30 29	0.30	747 (744)	39 (39)	3.1	5.8	15.98	B_T(RC3)
			55 27 47	0.71	12	12	0.5			RC3
MRK 408		UvES	09 45 07	0.74	1564 (1556)	92 (83)	2.7	3.5	14.86	m_B(RC3)
			33 06 52	0.47	20	20	0.4			SDAH00
MRK 27	UGCA 206	UvES	10 08 31	0.31	2098 (2094)	110 (102)	1.8	2.5	16.62	TM81
			58 58 01	0.55	16	16	0.3			RC3
MRK 32	UGCA 211	UvES	10 23 48	0.35	840 (841)	77 (67)	3.3	5.3	16.14	B_T(RC3)
			56 31 01	0.56	14	14	0.6			RC3
TOL 1108+098	Fairall 6	EmL	11 08 30	0.55	1587 (1588)	105 (98)	2.8	3.9	15.83	DCC99
			09 54 15	0.71	20	20	0.5			DCC99
UM 422	UGC 6345	EmL	11 17 39	2.34	1592 (1597)	96 (96)	21.8	8.1	13.80	B_T(RC3)
			02 48 16	0.55	10	10	1.7			RC3

Table 1. (continued)

(1) Galaxy	(2) Alternative name(s)	(3) Type	(4) R.A. Dec. (B1950)	(5) D'_{25} r_{25}	(6) $V_{\rm Hel}$ σ km s^{-1}	(7) W_{50} σ km s^{-1}	(8) FI σ Jy km s^{-1}	(9) $\sigma_{\rm RMS}$ channel^{-1} mJy	(10) B_T mag.	(11) Mag. ref. Diam. ref.
MRK 170	UGC 6448,	UvES	11 23 55	1.05	989 (987)	86 (74)	5.2	3.4	14.91	m_B(RC3)
			64 24 46	0.44	10	10	0.5			RC3
TOL 1124+090	IC 2828	EmL	11 24 48	1.32	1039 (1043)	48 (51)	2.0	3.3	14.38	m_B(RC3)
			09 00 30	0.44	12	12	0.4			RC3
UM 439	UGC 6578 Galaxy pair	EmL	11 34 02	1.07	1099 (1100)	93 (95)	7.0	3.2	15.03	CMM93
			01 05 38	0.30	12	12	0.5			UGC
UM 446		EmL	11 39 12	0.28	1802 (1797)	132 (133)	1.3	2.2	16.79	CMM93
			–01 37 26	0.93	14	14	0.3			SDAH00
UM 452		EmL	11 44 26	0.78	1439	–	–	5.6	14.90	m_B(RC3)
			–00 00 57	0.52						GPPMR96
UM 454		EmL	11 45 43	0.35	3870 (3866)	44 (50)	0.8	6.4	16.51	CMM93
			–01 21 43	0.57						SDAH00
UM 455	3.6′ from UM 456,	EmL	11 47 49	0.43	3863	–	–	5.5	17.10	CMM93
	separated in velocity		–00 15 01	0.63						GPPMR96
UM 456	3.6′ from UM 455	EmL	11 48 01	0.77	1757 (1767)	184 (181)	3.9	3.1	15.20	m_B(RC3)
	Two velocity components		–00 17 23	0.61	12	12	0.6			SDAH00
UM 461		EmL	11 48 59	0.46	1044 (1046)	81 (71)	3.0	4.1	16.20	DCC99
			–02 05 40	0.75	12	12	0.5			DCC99
UM 462	UGC 6850, MRK 1307	EmL	11 50 03	0.65	1055 (1052)	69 (67)	5.6	7.5	14.50	m_B(RC3)
		UvES	–02 11 26	0.85	12	12	0.8			RC3
UM 463		EmL	11 50 13	0.22	1199	–	–	3.7	17.87	CMM93
			–00 23 26	0.89						SDAH00
UM 465	IC 745, UGC 6877,	EmL	11 51 38	0.66	1145	–	–	3.5	14.20	m_B(RC3)
	MRK 1308, AK 332	UvES	00 24 56	0.93						RC3
UM 476	NGC 4116, UGC 7111	EmL	12 05 05	3.80	1309 (1312)	206 (206)	45.3	7.1	12.41	B_T(RC3)
	MRK 1466	UvES	02 58 32	0.58	4	4	2.9			RC3
UM 477	NGC 4123, UGC 7116,	EmL	12 05 36	4.37	1326 (1325)	200 (201)	55.2	12.9	11.98	B_T(RC3)
	MRK 1466	UvES	03 09 21	0.74	4	4	4.0			RC3
MRK 199	UGC 7168	UvES	12 08 04	1.17	2101 (2096)	123 (122)	6.6	8.8	15.43	m_B(RC3)
	2.9′ from UGC 07160		70 38 47	0.20	24	24	1.3			RC3
UM 483	MRK 1313	EmL	12 09 41	0.35	2328 (2326)	81 (88)	1.6	2.1	15.96	CMM93
		UvES	00 21 00	0.67	20	20	0.4			SDAH00
MRK 1315	1.4′ from NGC 4204	UvES	12 12 46	1.17	859 (860)	84 (84)	27.0	4.0	14.51	GPPMR96
			20 55 06	0.57	4	4	1.5			GPPMR96
MRK 1318	UGC 7534, MRK 49	UvES	12 16 36	0.68	1524 (1525)	55 (55)	2.6	4.0	14.00	B_T(RC3)
			04 07 57	0.85	12	12	0.5			RC3
UM 491		EmL	12 17 18	0.74	2025	–	–	6.7	16.73	GPPMR96
			02 03 02	0.38						GPPMR96
UM 499	NGC 4385, UGC 7515,	EmL	12 23 09	2.19	2145 (2152)	113 (109)	4.3	4.5	13.20	B_T(RC3)
	MRK 52	UvES	00 50 57	0.63	12	12	0.6			RC3
UM 500	UGC 7531	EmL	12 23 39	1.15	2031 (2035)	103 (109)	7.6	9.8	13.91	GPPMR96
	4.0′ from UM 501		–01 01 41	1.00	15	15	1.4			GPPMR96
UM 501	4.0′ from UM 500	EmL	12 23 48	0.44	2027 (2025)	111 (111)	6.5	4.5	16.80	GPPMR96
			–00 58 32	0.30	10	10	0.8			GPPMR96
UM 504		EmL	12 29 48	0.29	2086	–	–	3.1	16.46	CMM93
			–01 27 51	1.00						SDAH00
UM 505	UGC 7694, NGC 4437	EmL	12 30 11	10.47	1131 (1128)	305 (306)	33.5	10.3	11.10	B_T(RC3)
			00 23 25	0.15	2	2	2.5			RC3
UM 506	NGC 4536, UGC 7732	EmL	12 31 58	7.59	1799 (1807)	324 (324)	79.1	5.9	11.16	B_T(RC3)
			02 27 46	0.43	3	3	4.0			RC3
UM 513		EmL	12 39 26	0.30	3598	–	–	5.6	17.08	CMM93
			01 01 40	0.62						SDAH00
UM 514	NGC 4632, UGC 7870	EmL	12 39 57	3.09	1718 (1720)	219 (218)	39.5	6.3	12.36	m_B(RC3)
			00 11 31	0.38	4	4	2.5			RC3

Table 1. (continued)

(1) Galaxy	(2) Alternative name(s)	(3) Type	(4) R.A. Dec. (B1950)	(5) D'_{25} r_{25}	(6) $V_{\rm Hel}$ σ km s^{-1}	(7) W_{50} σ km s^{-1}	(8) FI σ Jy km s^{-1}	(9) $\sigma_{\rm RMS}$ channel^{-1} mJy	(10) B_T mag.	(11) Mag. ref. Diam. ref.
UM 523	UGC 8034	EmL	12 52 18	1.74	921 (913)	131 (101)	14.7	13.4	14.36	m_B(RC3)
	NGC 4809/10 Galaxy Pair		02 55 28	0.41	10	10	2.4			RC3
UM 525	UGC 8041	EmL	12 52 36	3.10	1321 (1324)	190 (189)	22.2	7.5	12.62	m_B(RC3)
			00 23 58	0.60	6	6	1.9			RC3
UM 533	UGC 8105	EmL	12 57 24	1.14	881 (885)	41 (38)	1.7	5.7	14.73	GPPMR96
			02 19 10	0.52	12	12	0.4			GPPMR96
UM 538		EmL	13 00 07	0.27	896	–	–	6.6	18.24	TBGS95
			01 20 31	0.57						SDAH00
MRK 450	Galaxy Group	UvES	13 12 29	0.95	863 (859)	58 (63)	3.2	3.4	14.75	m_B(RC3)
	UGC 8323		35 08 42	0.79	8	8	0.4			RC3
UM 559		EmL	13 15 08	0.45	1245 (1247)	111 (102)	5.1	4.1	16.90	GPPMR96
			–00 44 13	0.48	10	10	0.5			GPPMR96
UM 588		EmL	13 32 00	0.74	3897	–	–	6.6	15.38	GPPMR96
			–00 05 48	1.00						GPPMR96
UM 598	NGC 5257, UGC 8641	EmL	13 37 18	1.78	6798	–	–	5.2	13.36	B_T(RC3)
	1.3′ from NGC 5258		01 05 32	0.52						RC3
MRK 277	UGCA 375 Galaxy Pair	UvES	13 50 25	0.66	1755 (1758)	139 (124)	7.1	4.2	15.84	m_B(RC3)
			64 37 07	0.32	14	14	0.7			RC3
UM 626		UvES	13 58 09	1.07	3457 (3448)	94 (58)	1.3	2.9	14.97	GPPMR96
			–00 15 52	0.50	20	20	0.3			GPPMR96
NGC 5669	UGC 9353	G	14 30 17	3.98	1385 (1372)	200 (198)	44.4	13.0	12.03	m_B(RC3)
			10 06 36	0.71	6	6	3.5			RC3
1501+00		BCD	15 01 24	0.50	1588 (1592)	43 (37)	0.9	3.6	16.3	KKR99
			00 37 00	0.70	6	6	0.3			SDAH00
UM 167	NGC 7714, UGC 12699,									
	MRK 0538	EmL	23 33 40	1.91	2799 (2798)	182 (184)	22.8	5.1	13.00	B_T(RC3)
	2.0′ from NGC 7715	UvES	01 52 30	0.74	6	6	1.5			RC3

2.4. Derived properties

The derived properties are listed in Table 3 for the EmLGs and BCGs, and in Table 4 for the gas–rich irregulars. We assume H_0=75 km s^{-1} Mpc^{-1} and q_0=0. The column entries are as follows;

(1) Galaxy identification.
(2) Velocity in km s^{-1} corrected to the centre of the Local Group, $V_{\rm LG}$,

$$V_{\rm LG} = V_{\rm Hel} + 300 \times \sin(l) \times \cos(b) \ {\rm km\ s^{-1}}, \quad (1)$$

where l and b are the Galactic longitude and latitude respectively.
(3) Distance in Mpc, D calculated from $V_{\rm LG}$. No attempt has been made to correct for Virgocentric infall.
(4) Linear diameter in kpc derived from D'_{25}.
(5) Absolute blue magnitude, M_B corrected for Galactic extinction but not for internal absorption.
(6) Galactic extinction estimated from A_B=–0.2|cosec(b)| mag.
(7) Blue luminosity in 10^8 L$_\odot$, L_B, calculated assuming the absolute blue magnitude of the Sun is M$_B$=5.41 (Lang 1974).
(8) Beam corrected H I flux density integral in Jy km s^{-1}, $FI_{\rm c}$. Here $FI_{\rm c}$=$f_{\rm c} \times FI$, where $f_{\rm c}$ is given by

$$f_{\rm c} = (1 + (a_{HI}/\theta)^2)^{1/2}(1 + (b_{HI}/\theta)^2)^{1/2},$$

where θ is the full width half maximum of the telescope beam (12 arcmin for the Lovell Telescope) and a_{HI} and b_{HI} are the major and minor axes of the FWHM of the H I distribution which is assumed to be Gaussian.

a_{HI} and b_{HI} are taken to be the optical sizes at D'_{25} which is probably an underestimate. However, due to the small angular size of the majority of the sample galaxies, any error in the adopted H I-to-optical diameter ratio are only likely to contribute a few percent to the error in the beam-corrected H I flux density integral.
(9) H I mass in 10^8 M$_\odot$, M_{HI}, calculated from

$$M_{HI} = 2.36 \times 10^5 \times FI_c \times D^2 M_\odot.$$

This assumes that the H I in galaxies is optically thin to its own radiation (Staveley-Smith & Davies 1987 although see de Vaucouleurs et al. 1991).
(10) H I mass to blue luminosity ratio, M_{HI}/L_B in solar units M$_\odot$/L$_\odot$.
(11) If the galaxy is isolated then there is a 'Y' in this column, otherwise a 'N'.

Table 2. Observational data for the gas–rich irregular galaxy sample.

(1) Galaxy	(2) Alternative name(s)	(3) Type	(4) R.A. Dec. (B1950)	(5) D'_{25} r_{25}	(6) $V_{\rm Hel}$ σ km s^{-1}	(7) W_{50} σ km s^{-1}	(8) FI σ Jy km s^{-1}	(9) $\sigma_{\rm RMS}$ channel^{-1} mJy	(10) B_T mag.	(11) Mag ref. Diam. ref
UGC 17	DDO 222	Sm:	00 01 07	2.45	879 (878)	98 (99)	5.4	2.6	14.80	B_T(RC3)
			14 56 12	0.71	12	12	1.1			RC3
UGC 47		Sdm:	00 04 04	1.28	877 (876)	88 (88)	4.5	2.7	17	UGC
			17 00 20	0.15	4	4	0.4			RC3
UGC 119		S?	00 10 28	1.00	2022 (2027)	85 (83)	6.4	3.5	14.60	SAD99
			14 07 58	0.62	10	10	0.6			RC3
UGC 772		Im:	01 11 06	1.20	1172 (1164)	44 (41)	5.0	16.2	16.11	SAD99
			00 36 42	0.76	10	10	0.6			RC3
UGC 1104		Im	01 30 01	1.00	684 (685)	89 (84)	11.2	4.2	14.41	SAD99
			18 03 33	0.63	6	6	0.9			RC3
DDO 36		SB(s)m	05 05 31	2.34	2036 (2037)	36 (36)	13.8	5.8	13.80	SAD99
			–16 21 41	0.59	4	4	1.0			RC3
UGC 3409		Sm:	06 05 57	1.48	1361 (1360)	123 (119)	8.8	3.3	17	UGC
			64 34 33	0.28	10	10	0.7			RC3
UGC 4660		Sm:	08 51 17	1.17	2202 (2202)	58 (58)	7.6	4.7	15.37	SAD99
			34 44 50	0.93	6	6	0.6			RC3
DDO 62	UGCA 162	IB(s)m	09 19 12	2.51	849 (847)	124 (126)	33.1	8.0	14.7	SAD99
			–22 17 18	0.23	4	4	2.0			RC3
UGC 5571		Sm:	10 16 36	1.17	662 (662)	44 (44)	8.0	3.4	15.77	SAD99
			52 20 00	0.32	4	4	0.5			RC3
UGC 6669		Im	11 39 43	1.45	1021 (1019)	68 (66)	7.2	6.0	15.2	UGC
			15 16 30	0.51	8	8	0.8			RC3
DDO 123	UGC 7534,	IBm	12 23 46	2.63	724 (725)	58 (58)	25.4	7.8	14.50	m_B(RC3)
			58 35 47	0.79	2	2	1.7			RC3
UGC 7745		Im:	12 32 39	1.00	1186 (1188)	74 (71)	1.3	3.1	17	UGC
			73 56 27	0.65	15	15	0.4			RC3
DDO 153	UGCA 307	IB(s)m	12 51 20	2.00	824 (824)	67 (66)	22.2	10.1	14.58	SAD99
			–11 50 14	0.50	3	3	1.7			RC3
UGC 8127C		IB(s)m	12 58 26	1.55	1447 (1468)	147 (148)	8.7	4.9	14.73	m_B(RC3)
			–01 42 00	0.30	6	6	1.0			RC3
DDO 171		IB(s)m	13 16 04	1.70	1305 (1307)	44 (44)	5.2	4.8	14.02	B_T(RC3)
			–08 11 00	0.72	6	6	0.6			RC3
UGC 8639		Im:	13 37 00	1.48	1690 (1689)	122 (122)	4.5	4.5	14.67	SAD99
			51 42 00	0.74	10		0.6			RC3
UGC 8936		Im:	13 58 59	1.29	1907 (1911)	164 (101)	6.2	3.2	17	UGC
			49 36 53	0.78	16	16	0.6			RC3
UGC 9046		Im:	14 06 33	1.10	2099 (–)	425 (392)	7.0	2.9	16.70	SAD99
			48 12 20	0.66	16	16	0.7			RC3
UGC 9426		Im	14 35 42	1.51	2306 (2308)	46 (46)	5.1	6.5	15.85	SAD99
			48 49 00	0.63	6	6	0.6			RC3
DDO 195		IB(s)m	14 36 14	2.88	1824 (1828)	61 (62)	10.4	5.4	15.1	DDB83
			–08 24 53	0.25	6	6	0.9			RC3
UGC 10991	VII Zw741	Im	17 46 36	1.05	1461 (1457)	48 (48)	4.7	3.8	15.29	SAD99
			67 21 00	0.83	4	4	0.5			RC3
DDO 215	UGCA 433	Im:	22 36 34	1.70	829 (831)	60 (58)	7.6	3.4	14.97	B_T(RC3)
			–05 01 27	0.30	4	4	0.5			RC3
UGC 12846		Sm:	23 53 18	1.82	1734 (1734)	96 (92)	7.8	3.8	15.58	SAD99
			18 10 00	0.91	3	3	0.6			RC3

Table 3. Analyzed data for the EmLG and BCD galaxy sample.

(1) Galaxy	(2) V_{LG} km s^{-1}	(3) D Mpc	(4) Diam. kpc	(5) M_B mag.	(6) A_B mag.	(7) L_B $\times 10^8 L_\odot$	(8) FI_c Jy km s^{-1}	(9) M_{HI} $\times 10^8 M_\odot$	(10) M_{HI}/L_B $M_\odot/L_\odot$	(11) Isolated?
UM 38	1524	20.3	3.7	–16.27	–0.23	4.71	2.6	2.53	0.54	Y
UM 69	2085	27.8	7.7	–17.28	–0.23	12.0	5.2	9.48	0.79	Y
UM 285	2015	26.9	2.4	–15.04	–0.23	1.52	1.0	1.70	1.12	Y
UM 304	4819	64.3	12.9	–18.87	–0.23	51.5	–	–	–	Y
UM 306	5023	67.0	9.5	–18.16	–0.23	26.8	2.5	26.5	0.99	N
UM 307	6867	91.6	26.6	–20.73	–0.23	285	3.3	65.3	0.23	Y
UM 309	1255	16.7	17.9	–19.45	–0.23	87.6	74.0	48.9	0.56	Y
UM 311	1854	24.7	23.9	–19.55	–0.22	96.3	21.8	31.4	0.33	Y
UM 318	2445	32.6	32.1	–19.86	–0.23	129	36.2	90.8	0.70	Y
UM 323	2009	26.8	3.6	–16.42	–0.23	5.37	2.4	4.06	0.76	Y
UM 111	2068	27.6	8.8	–18.56	–0.24	38.8	10.8	19.4	0.50	N
UM 343	5244	69.9	37.0	–20.74	–0.23	289	–	–	–	Y
UM 133	1713	22.8	6.2	–16.66	–0.24	6.71	4.2	5.17	0.77	Y
UM 137	1881	25.1	8.4	–17.49	–0.24	14.4	4.5	6.68	0.46	Y
UM 372	1768	23.6	7.2	–17.29	–0.24	12.0	3.6	4.72	0.39	Y
UM 382	3661	48.8	3.4	–15.12	–0.23	1.62	–	–	–	Y
UM 404	3627	48.4	20.5	–15.26	–0.24	1.85	6.2	34.2	18.50	N
UM 408	3568	47.6	3.6	–16.05	–0.24	3.84	1.5	8.01	2.08	Y
UM 417	2740	36.5	2.9	–14.85	–0.24	1.27	–	–	–	Y
UM 418	7784	104	34.7	–21.02	–0.24	374	2.5	63.6	0.17	Y
MRK 600	1049	14.0	2.3	–15.53	–0.27	2.38	5.8	2.68	1.13	Y
I Zw 18	818	10.9	1.0	–14.49	–0.28	0.91	3.1	0.87	0.95	Y
MRK 408	1520	20.3	4.4	–16.93	–0.26	8.66	2.7	2.62	0.30	Y
MRK 27	2190	29.2	2.6	–15.98	–0.27	3.58	1.8	3.62	1.01	N
MRK 32	921	12.3	1.3	–14.56	–0.26	0.98	3.3	1.17	1.20	Y
Tol 1108+098	1454	19.4	3.1	–15.84	–0.23	3.15	2.8	2.48	0.79	Y
UM 422	1433	19.1	13.0	–17.84	–0.24	20.0	21.8	18.8	0.94	Y
MRK 170	1118	14.9	4.6	–16.22	–0.26	4.47	5.3	2.78	0.62	Y
Tol 1124+090	909	12.1	4.7	–16.26	–0.22	4.67	2.0	0.69	0.15	Y
UM 439	941	12.5	3.9	–15.70	–0.24	2.77	7.0	2.60	0.94	N
UM 446	1637	21.8	1.8	–15.14	–0.24	1.67	1.3	1.46	0.88	Y
UM 452	1282	17.1	3.9	–16.50	–0.23	5.80	0.9	–	–	Y
UM 454	3759	50.1	5.1	–17.23	–0.24	11.4	0.8	4.74	0.42	Y
UM 455	3707	49.4	6.2	–16.60	–0.23	6.39	–	–	–	Y
UM 456	1601	21.3	4.8	–16.68	–0.23	6.86	3.9	4.19	0.61	N
UM 461	882	11.8	1.4	–14.39	–0.24	0.83	3.0	0.98	1.18	Y
UM 462	893	11.9	2.3	–16.12	–0.24	4.08	5.6	1.87	0.46	Y
UM 463	1044	13.9	0.9	–13.08	–0.23	0.25	–	–	–	Y
UM 465	994	13.3	2.5	–16.64	–0.23	6.63	–	–	–	Y
UM 476	1176	15.7	17.3	–18.79	–0.22	47.9	43.7	25.4	0.53	Y
UM 477	1194	15.9	20.2	–19.25	–0.22	73.3	54.0	32.3	0.44	Y
MRK 199	2265	30.2	10.3	–17.25	–0.28	11.6	5.0	10.8	0.93	N
UM 483	2188	29.2	3.0	–16.59	–0.23	6.33	1.6	3.21	0.51	Y
MRK 1315	808	10.8	3.7	–15.86	–0.20	3.21	27.0	7.40	2.31	Y
MRK 1318	1403	18.7	3.7	–17.58	–0.22	15.7	2.7	2.23	0.14	Y
UM 491	1896	25.3	5.4	–15.51	–0.22	2.33	–	–	–	Y
UM 499	2015	26.9	17.1	–19.17	–0.23	68.0	4.3	7.33	0.11	Y
UM 500	1894	25.3	8.4	–18.33	–0.23	31.3	7.6	11.4	0.36	N
UM 501	1890	25.2	3.2	–15.44	–0.23	2.18	6.2	9.29	4.26	N
UM 504	1951	26.0	2.2	–15.85	–0.23	3.18	–	–	–	Y
UM 505	1003	13.4	40.7	–19.76	–0.23	117	133.5	56.4	0.48	Y
UM 506	1681	22.4	49.5	–20.81	–0.22	309	68.3	82.0	0.26	Y
UM 513	3479	46.4	4.0	–16.48	–0.22	5.68	–	–	–	Y
UM 514	1597	21.3	19.1	–19.51	–0.23	92.6	39.5	42.3	0.46	Y
UM 523	819	10.9	5.5	–16.05	–0.22	3.84	14.7	4.14	1.08	N

Table 3. (continued)

(1) Galaxy	(2) V_{LG} km s^{-1}	(3) D Mpc	(4) Diam. kpc	(5) M_B mag.	(6) A_B mag.	(7) L_B $\times 10^8$L$_\odot$	(8) FI_c Jy km s^{-1}	(9) M_{HI} $\times 10^8$M$_\odot$	(10) M_{HI}/L_B M$_\odot$/L$_\odot$	(11) Isolated?
UM 525	1210	16.1	14.5	–18.64	–0.22	41.8	22.2	13.6	0.33	Y
UM 533	780	10.4	3.4	–15.58	–0.22	2.48	1.7	0.43	0.17	Y
UM 538	794	10.6	0.8	–12.60	–0.22	0.19	–	–	–	Y
MRK 450	913	12.2	3.4	–15.88	–0.20	3.28	3.2	1.12	0.34	N
UM 559	1145	15.3	2.0	–14.25	–0.23	0.73	5.1	2.81	3.85	Y
UM 588	3813	50.8	10.9	–18.38	–0.23	32.8	–	–	–	Y
UM 598	6723	89.6	46.4	–21.63	–0.23	655	–	–	–	N
MRK 277	1927	25.7	4.9	–16.46	–0.26	5.62	7.1	11.1	1.97	N
UM 626	3394	45.3	14.1	–18.54	–0.24	38.2	1.3	6.28	0.16	Y
NGC 5669	1390	18.5	21.5	–19.54	–0.23	95.5	44.4	36.0	0.38	Y
1501+00	1576	21.0	4.9	–15.58	–0.27	2.49	1.0	1.04	0.42	Y
UM 167	2969	39.6	22.0	–20.23	–0.24	180	22.8	84.2	0.47	N

Table 4. Analyzed data for the gas-rich irregular galaxy sample.

(1) Galaxy	(2) V_{LG} km s^{-1}	(3) D Mpc	(4) Diam. kpc	(5) M_B mag.	(6) A_B mag.	(7) L_B $\times 10^8$L$_\odot$	(8) FI_c Jy km s^{-1}	(9) M_{HI} $\times 10^8$M$_\odot$	(10) M_{HI}/L_B M$_\odot$/L$_\odot$	(11) Isolated?
UGC 17	1079	14.4	10.3	–16.26	–0.27	4.67	5.4	2.64	0.56	Y
UGC 47	1081	14.4	5.4	–14.08	–0.29	0.63	4.5	2.21	3.53	Y
UGC 119	2214	29.5	8.6	–18.02	–0.27	23.6	6.4	13.2	0.56	Y
UGC 772	1251	16.7	5.8	–15.23	–0.23	1.80	5.0	3.28	1.82	Y
UGC 1104	834	11.1	3.2	–16.31	–0.29	4.88	11.2	3.27	0.67	Y
DDO 36	1881	25.1	17.1	–18.60	–0.40	40.1	13.8	20.5	0.51	Y
UGC 3409	1503	20.0	8.6	–15.09	–0.58	1.59	8.8	8.34	5.26	N
UGC 4660	2165	28.9	9.8	–17.82	–0.32	19.6	7.6	15.0	0.76	Y
DDO 62	579	7.7	5.6	–15.35	–0.60	2.01	33.1	4.66	2.31	Y
UGC 5571	721	9.6	3.3	–14.40	–0.25	0.84	8.0	1.74	2.08	Y
UGC 6669	926	12.3	5.2	–15.47	–0.21	2.25	7.2	2.59	1.15	Y
DDO 123	846	11.3	8.6	–16.00	–0.23	3.65	25.4	7.63	2.09	Y
UGC 7745	1366	18.2	5.3	–14.59	–0.29	1.00	1.4	1.10	1.09	N
DDO 153	666	8.9	5.2	–15.41	–0.25	2.14	22.2	4.13	1.93	Y
UGC 8127C	1332	17.8	8.0	–16.74	–0.23	7.27	8.7	6.48	0.89	N
DDO 171	1179	15.7	7.8	–17.21	–0.25	11.2	5.2	3.03	0.27	Y
UGC 8639	1688	22.5	9.7	–17.31	–0.22	12.3	4.6	5.50	0.45	Y
UGC 8936	2037	27.2	10.2	–15.39	–0.22	2.09	6.4	11.1	5.32	Y
UGC 9046	2229	29.7	9.5	–15.89	–0.22	3.30	7.0	14.6	4.42	Y
UGC 9426	2454	32.7	14.4	–16.95	–0.23	8.83	5.1	12.9	1.46	Y
DDO 195	1762	23.5	19.7	–16.93	–0.28	8.64	10.4	13.6	1.57	Y
UGC 10991	1715	22.9	7.0	–15.48	–0.39	2.28	4.7	5.80	2.55	Y
DDO 215	995	13.3	6.6	–15.90	–0.26	3.34	7.6	3.16	0.94	Y
UGC 12846	1948	26.0	13.8	–16.79	–0.30	7.58	7.8	12.4	1.64	Y

3. Results

3.1. H I content

3.1.1. A note concerning companions

The prime aim of this study was to determine the H I mass to blue luminosity ratio of EmLGs for comparison with UV-excess selected galaxies. Before discussing the results, it is important to note that these observations were taken with a single dish and thus the observed H I profiles may be contaminated by companions. In an effort to reduce this contamination, we searched for companion galaxies within a radius of 15 arcmin of the main galaxy using the NASA extragalactic database. Where a companion object was found at the same redshift of the main galaxy, its contribution to the observed single-dish H I mass of the main object was estimated using the angular distance from the main galaxy, type and optical magnitude of the companion. When the estimated fractional mass contribution from the companion exceeded 5% of the H I mass of the main galaxy, we eliminated it from our sample.

Aside from optical companions, H I synthesis observations by Taylor et al. (1993,1995) have shown that many H II galaxies have previously uncatalogued optically undetected H I companions. All of the 20 galaxies observed using H I-synthesis by Taylor et al. (1995) are common to our sample. Taylor et al. (1995) found that over half of these objects have an H I companion. However, within the 38 UM EmLGs that we detected in H I within our current sample, we only observe an obvious H I companion to a single galaxy, UM 456. There are four reasons why we do not detect more companion objects. In some cases (e.g. UM numbers 323, 461, 462, 477) the companion is of order 15 arcmin away from the main galaxy at which point the beam response of the Lovell Telescope is less than 2% of the peak. Other companions are closer but much fainter than the main object (e.g. UM 422, UM 483). A few companions may lie outside of the observed velocity range in the case of the observations of bandwidth 5 MHz. Finally in systems such as UM 500/501, the H I velocities and coordinates of the two UM objects are similar, resulting in an H I profile that is difficult to distinguish from that of an isolated galaxy.

The presence of uncatalogued close companions of similar redshift to the main object could increase the observed M_{HI}/L_B ratios of the sample galaxies, particularly in the case of the dwarf galaxies in the sample. However, comparing our single-dish H I results with those of Taylor et al. (1995) shows that only in the UM 500/501 pair are our H I masses significantly greater. This pair had previously been removed from our sample in any case by virtue of their optical identifications. Hence in the following discussion we assume that our galaxies without optical companions are essentially isolated with respect to the Lovell Telescope beam.

3.1.2. Hydrogen mass and M_{HI}/L_B ratios

There is a large range in both the H I masses and the M_{HI}/L_B ratios of the EmLGs in the present sample. For the 14 objects where H I was not detected by the current observations, we performed a literature search to find H I masses. H I masses for UM numbers 452, 465, 491, 504, 538 were taken from Taylor et al. (1995); for UM 343 from Haynes & Giovanelli (1984) and for UM 455 from Huchtmeier et al. (1997). For the plots, the H I masses for the close pair UM numbers 500,501 are taken from the synthesis data of Taylor et al. (1995) and not from our single-dish observations. Hence of the original 52 UM galaxies, 6 have no H I data available and 8 are not isolated. This leaves 38 galaxies (including UM 500/501) for which we have reliable M_{HI}/L_B ratios.

Fig. 3 depicts a histogram of the H I masses of the isolated UM galaxy sample in which we detected gas. The H I mass for these objects varies from $\sim 4\times10^7$M$_\odot$ to 9×10^9 M$_\odot$ with the peak of the distribution at $\sim 6\times10^8$ M$_\odot$. These values are similar to the results of Thuan et al. (1999) for a sample of blue compact galaxies selected using objective-prism techniques.

For the objects where H I was detected, the galaxy with the lowest value of M_{HI}/L_B is UM 499, a large starburst galaxy which has M_{HI}/L_B=0.11 M$_\odot$/L$_\odot$ and M_B=–19.2. The galaxy with highest H I mass to blue luminosity ratio is the dwarf galaxy UM 559 which has M_{HI}/L_B=3.9 M$_\odot$/L$_\odot$ and M_B=–14.3.

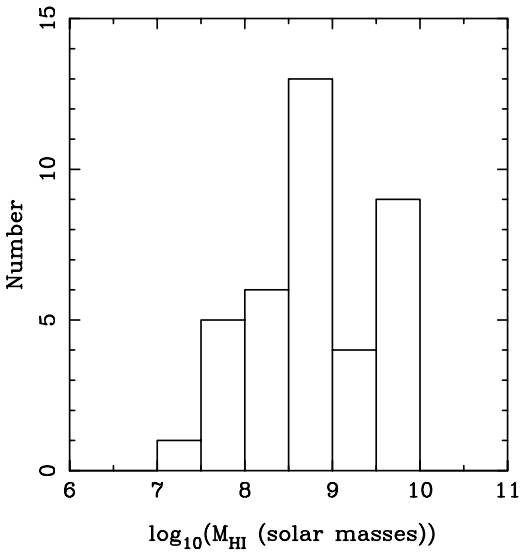

Fig. 3. Histogram of H I masses for isolated galaxies taken from the University of Michigan emission-line sample.

3.1.3. M_{HI}/L_B as a function of blue luminosity for EmLGs

Fig. 4 shows the H I mass to blue luminosity ratio plotted against absolute blue magnitude for both the UM EmL and UV-excess selected galaxies in the sample. Also plotted are the isolated UV-excess selected Markarian galaxies from TM81.

For the galaxies detected in H I, Fig. 4 suggests that there is a slight tendency for dwarf EmLGs to be more gas-rich than their brighter counterparts. Of course, this plot may be affected by selection effects; the gas-poor dwarfs being the hardest galaxies to detect in the first place. However, of the isolated sample galaxies without an available H I mass, only 4/6 are fainter than M_B=–17 compared to 18/38 of the detected objects. Hence the observed trend in increasing M_{HI}/L_B ratio with decreasing luminosity appears to be real. A fit of $M_{HI}/L_B \propto L_B^\beta$ to the H I-detected UM EmLG data gives β=–0.2$\pm$0.1.

3.1.4. Comparison with other surveys

The trend of increasing M_{HI}/L_B with decreasing luminosity has been noted by several previous authors; for low surface brightness dwarf irregular galaxies (Fisher & Tully 1975); spiral galaxies (Huchtmeier & Richter 1988); and LSB dI and BCGs (Staveley–Smith et al. 1992). We have reanalyzed the LSB dI data from Fisher & Tully (1975) (LSB dIs), and the BCG data from Gordon & Gottesman (1981) and Thuan & Martin (1981) using only photoelectric magnitudes taken from RC3 and find values of β of –0.3$\pm$0.06, –0.1$\pm$0.1 and –0.3$\pm$0.1 respectively. These values are in agreement with Staveley-Smith et al. (1992) who find β=–0.3$\pm$0.1 for both LSB dIs and BCGs. If the observed increase in H I-richness with decreasing blue luminosity continues to fainter objects, this implies that there may exist

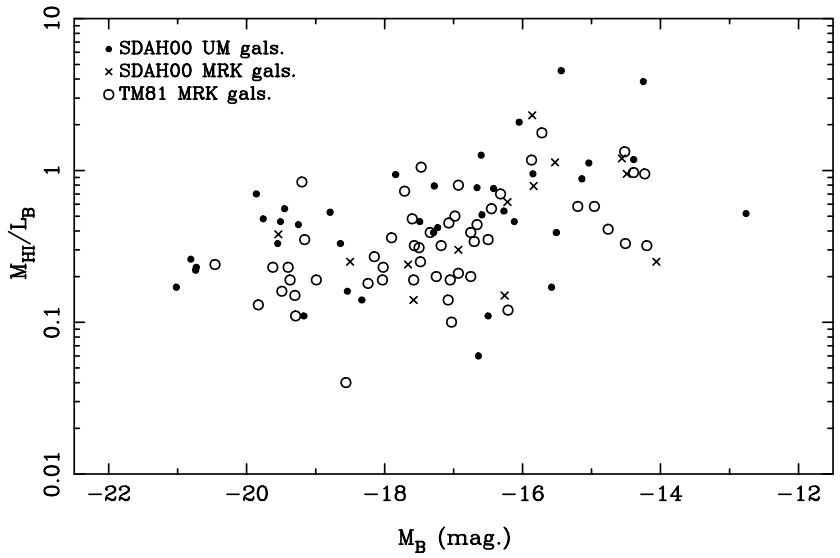

Fig. 4. H I mass to blue luminosity ratio plotted against absolute blue magnitude for University of Michigan emission-line galaxies (filled circles) and Markarian UV-excess galaxies (crosses) from the current sample and Markarian galaxies taken from TM81 (open circles).

optically-faint galaxies with reservoirs of neutral hydrogen still available for star formation.

3.1.5. Comparing the M_{HI}/L_B ratios of emission-line and blue compact galaxies

In this section the relative H I-richness of emission-line and blue compact galaxies are compared. Fig. 4 suggests that the M_{HI}/L_B ratios of our observed UM objects (EmL-selected galaxies) are similar to our UV-excess selected Markarian galaxies of the same luminosity. Since the number of Markarian galaxies we observed is small, in Fig. 4 we compare our observed data with the corresponding UV-excess Markarian galaxies of Thuan & Martin (1981) (TM81). Optical data for the TM81 galaxies were taken from RC3 with no internal extinction corrections and A_B=–0.2|cosec(b)| mag. Seven galaxies from the Markarian catalogue are present in both the present sample and in TM81. Comparison of these H I data indicates that the flux density scales are the same although flux density integral values for individual galaxies vary by up to 25% in the two datasets. Comparing our UM EmLG data with the Markarian data of TM81 in Fig. 4, we find that the M_{HI}/L_B values of the EmLGs are slightly higher than those galaxies taken from the TM81 Markarian sample. However, clearly there is a lot of overlap between the two types and the difference in the median values in M_{HI}/L_B in the detected galaxies is probably not significant, being 0.46 $M_\odot/L_\odot$ for the EmLGs (n=38) and 0.31 $M_\odot/L_\odot$ for the TM81 MRK UV–excess galaxies (n=69). If we assume that the undetected galaxies have M_{HI}/L_B values lower than the median, the resulting median value for the whole UM EmLG sample falls to 0.45 $M_\odot/L_\odot$ (n=44), that for the Markarian sample remains unchanged at 0.31 $M_\odot/L_\odot$. Both samples have similar blue luminosity distributions. For comparison, van Zee et al. (1995) find that M_{HI}/L_B=0.5 $M_\odot/L_\odot$ for emission-line galaxies and M_{HI}/L_B=1.1 $M_\odot/L_\odot$ for EmLGs with extended H I.

It is noted that if we consider only those Markarian galaxies classed as H II galaxies by Mazzarella & Balzano (1986), the median M_{HI}/L_B is 0.36 $M_\odot/L_\odot$ (n=10), compared with 0.31 for the whole sample (n=69).

Figs. 5 and 6 plot the H I mass and blue magnitude against the optical diameters for both the current UM sample and for the TM81 Markarian-selected galaxies. Again there is a lot of scatter, although these figures tentatively indicate that at a constant diameter the blue luminosities of the Markarian UV-excess galaxies are higher than those of the emission-line galaxies (Fig. 6); the H I contents are similar (Fig. 5). This would be consistent with there being a higher level of star formation in the UV-excess selected galaxies than in the EmLGs over the last 10^9 years rather than the EmLGs being more gas-rich. However, it must be emphasised that due to the heterogenous nature of the optical data and the large overlap between the observables for the two galaxy types, the detected differences may not be significant.

3.2. The metallicity of the programme galaxies

Aside from the gas content, a further criterion used to investigate the evolutionary state of a galaxy is the metallicity; low metallicity objects are less evolved than their high metallicity counterparts. The decrease in metallicity with decreasing luminosity for emission-line galaxies is well established (e.g. Campos-Aguilar et al. 1993; Salzer et al. 1989b). Such a trend implies either that smaller galaxies are less able to retain their processed material than larger galaxies or they are less evolved as a class of objects. Here we compare the metallicity of the UM galaxies in our sample with their M_{HI}/L_B ratios. We would have expected *a priori* that objects with high M_{HI}/L_B ratios would be less evolved and hence have lower metallicities. Fig. 7 plots the metallicity 12+$\log_{10}$(O/H) against the M_{HI}/L_B ratio. The values of 12+$\log_{10}$(O/H) were taken from Campos-Aguilar et al. (1993) and Masegosa et al. (1994) with the H I masses and blue luminosities being from the current paper.

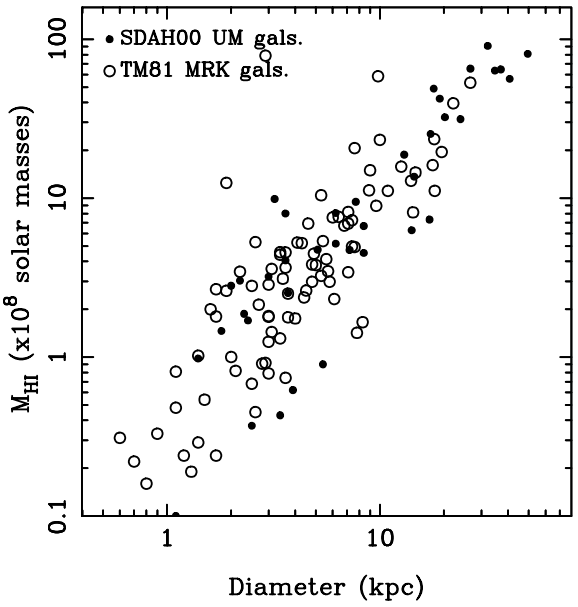

Fig. 5. H I mass plotted against diameter for the UM EmLGs from the present sample and for the Markarian UV-excess galaxies taken from Thuan & Martin (1981).

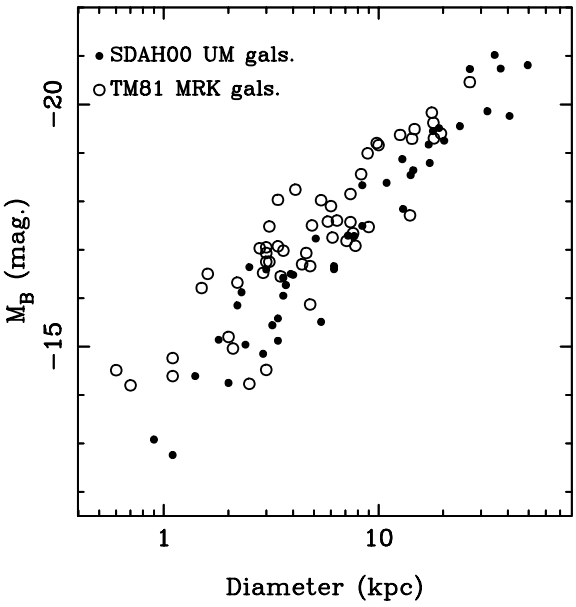

Fig. 6. Blue luminosity plotted against diameter for the UM EmLGs from the present sample and for the Markarian UV-excess galaxies taken from Thuan & Martin (1981).

As expected, decreasing metallicity is correlated with increasing H I mass to blue luminosity ratio which again indicates that searches for gas-rich systems may be a useful way of finding unevolved objects.

4. Discussion

4.1. The dependence of M_{HI}/L_B on L_B

We now consider the possible reasons for the increase in M_{HI}/L_B with decreasing luminosity found in Sect. 3.1.3. The increase traces a decline in recent star formation efficiency per unit mass with luminosity. The reason for this decrease has been discussed in Hoffman et al. (1992). Since the work of Searle & Sargent (1972) it has been thought that lower mass galaxies experience star formation in episodic 'bursts'. This 'bursting' has been described by the stochastic self-propagating star formation model of Gerola et al. (1980) (although see Brosch et al. 1998) and predicts that the bursts of star formation should become rarer as the galaxy mass is reduced. In the same vein, Tyson & Scalo (1988) suggest that the lowest mass galaxies may have only undergone a few bursts over their lifetimes and will thus be relatively faint optically with reservoirs of neutral hydrogen still available. The reason that the H I reservoirs are not converted to stars may be connected to the decrease in H I surface density with mass for irregular galaxies (Hoffman et al. 1989 although see Lo et al. 1993); late-type dwarf galaxies typically have peak H I surface densities a factor two lower than their brighter irregular counterparts. Given that star formation in spirals (Impey & Bothun 1989; Bothun et al. 1990), irregular galaxies (Skillman et al. 1987; Smoker 1993; van der Hulst et al. 1993) and H II galaxies (Taylor et al. 1994) does not occur beneath a limiting H I surface density of ~ 0.5–1.0×10^{20} n$_{HI}$ cm^{-2}, it naturally follows that dwarfs with low H I column density may have low star formation rates and thus have high M_{HI}/L_B ratios. There may thus exist extremely gas-rich dwarf galaxies faint in the optical as postulated by Tyson & Scalo (1988).

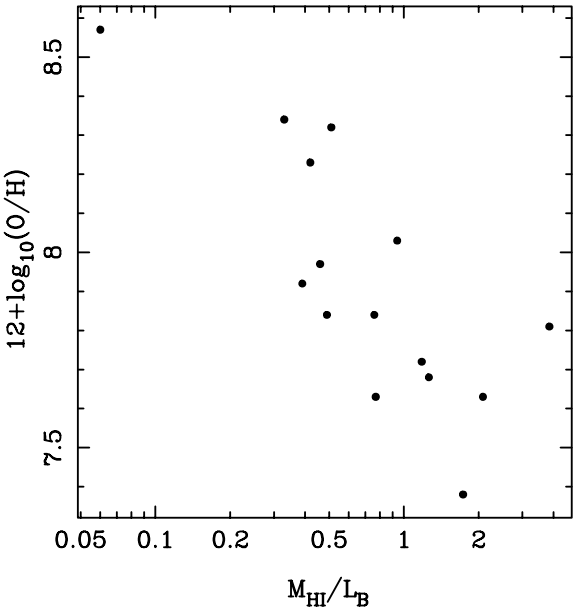

Fig. 7. Metallicity {12+log$_{10}$(O/H)} plotted against M_{HI}/L_B ratio for 15 University of Michigan emission-line galaxies.

5. Conclusions

We have observed a sample of emission-line galaxies from the University of Michigan catalogue and find that they have similar, although not identical H I properties to the blue compact

galaxies observed by Thuan & Martin (1981). Fractional neutral hydrogen contents are found to increase with decreasing luminosity following $M_{HI}/L_B \propto L_B^{-0.2}$

We finally note that the if the increase in M_{HI}/L_B ratio with decreasing luminosity is continued to lower luminosities, there may be exceedingly gas-rich dwarf galaxies undetected optically, as envisioned by Tyson & Scalo (1988). However, H I-searches for such dwarf galaxies in the field (e.g. Fisher & Tully 1981b; Briggs 1990) and in voids (Krumm & Brosch 1984; Hulsbosch 1987; Brosch 1989; Weinberg et al. 1991; Hoffman et al. 1992) have so far failed to find a significant population of such H I-rich, low optical-luminosity dwarfs (Briggs 1997), at least assuming that they fill the telescope beam and have H I column densities greater than $\sim 5{\times}10^{19}\ n_{HI}\ \mathrm{cm}^{-2}$.

Acknowledgements. We would like to thank John Salzer for supplying us with magnitudes of a number of the UM galaxies. JVS is grateful to PPARC for financial support. This research has made extensive use of the NASA/IPAC extragalactic database (NED), which is operated by the Jet Propulsion Laboratory, Caltech, under contract with NASA.

References

Balzano V.A., 1983, ApJ 268, 602
Bohuski T.J., Fairall A.P., Weedman D.W., 1978, ApJ 221, 776
Bothun G.D., Schombert J.M., Impey C.D., Schneider S.E., 1990, ApJ 360, 427
Briggs F.H., 1990, AJ 100, 999
Briggs F.H., 1997, ApJ 484, 29
Brosch N., 1989, ApJ 344, 597
Brosch N., Heller A., Almoznino E., 1998, MNRAS 300, 1091
Campos-Aguilar A., Moles M., Masegosa J., 1993, AJ 106, 1784
de Vaucouleurs G., de Vaucouleurs,A., Corwin Jr. H.G., 1976, Second reference catalogue of bright galaxies. University of Texas Press, Austin (RC2)
de Vaucouleurs G., de Vaucouleurs A., Corwin Jr. H.G., et al., 1991, Third Reference Catalogue of Bright Galaxies. Springer, New York (RC3)
de Vaucouleurs G., de Vaucouleurs, Buta R., 1983, AJ 88, 764
Doublier V., Caulet A., Comte G., 1999, A&AS 138, 213
Dreyer J.L.E., 1895 Mem. R. Astron. Soc. 51, 185
Dreyer J.L.E., 1888, Mem. R. Astron. Soc. 49, 1
Fisher J.R., Tully R.B., 1975, A&A 44, 151
Fisher J.R., Tully R.B., 1981a, ApJS 47, 139
Fisher J.R., Tully R.B., 1981b, ApJ 243, 23
French H.B., 1980, ApJ 240, 41
Garnier R., Paturel G., Petit C., Marthinet M.C., Rousseau J., 1996, A&AS 117, 467
Gerola H., Seiden P.E., Schulman L.S., 1980, ApJ 242, 517
Gordon D., Gottesman S.T., 1981, AJ 86, 161
Haro G., 1956, Bol. Obs. Tonantzintlay Tacubaya 14, 8
Haynes M.P., Giovanelli R., 1984, AJ 89, 758
Hoffman G.L., Helou G., Salpeter E.E., Lewis B.M., 1989, ApJ 339, 812
Hoffman G.L., Lu N.Y., Salpeter E.E., 1992, AJ 104, 2086
Huchra J.P., 1977, ApJS 35, 171
Huchtmeier W.K., Richter O.-G., 1988, A&A 203, 237
Huchtmeier W.K., Hopp U., Kuhn B., 1997, A&A 319, 67
Hulsbosch A.N.M., 1987, A&AS 69, 439
Impey C.D., Bothun G.D., 1989, ApJ 341, 89
Impey C.D., Sprayberry D., Irwin M.J., Bothun G.D., 1996, ApJS 105, 209
Karachentseva V.E., Karachentsev I.D., Richter G.M., 1999, A&AS 135, 221
Khachikian E.Ye., 1987, In: IAU symposium 121, Observational Evidence of Activity in Galaxies. p. 65
Krumm N., Brosch N., 1984, AJ 89, 1461
Lang K.R., 1974, Astrophysical Formulae. Springer, Berlin
Lo K.Y., Sargent W.L.W., Young K., 1993, AJ 106, 507
MacAlpine G.M., Lewis D.W., 1978, ApJS 36, 587
MacAlpine G.M., Williams G.A., 1981, ApJS 45, 113
Markarian B.E., 1967, Afz 3, 24
Markarian B.E., Lipovetskii V.A., Stepanian D.A., 1981, Afz 17, 619
Markarian B.E., Lipovetskii V.A., Stepanian D.A., 1983, Afz 19, 29
Markarian B.E., Lipovetsky V.A., Stepanian J.A., Erastova L.K., Shapovalova A.I., 1989, Comm. Special Ap. Obs. 62, 5
Masegosa J., Moles M., Campos-Aguilar C., 1994, ApJ 420, 576
Mazzarella J.M., Balzano V.A., 1986, ApJS 62, 751
Nilson P., 1973, Uppsala General Catalog of Galaxies. Royal Society of Sciences of Uppsala, Uppsala, Sweden
Pointon L., 1977, J. Phys. E. 10, 833
Salzer J.J., MacAlpine G.M., 1988, AJ 96, 1192
Salzer J.J., MacAlpine G.M., Boroson T.A., 1989a, ApJS 70, 447
Salzer J.J., MacAlpine G.M., Boroson T.A., 1989b, ApJS 70, 479
Searle L., Sargent W.L.W., 1972, ApJ 173, 25
Skillman E.D., Bothun G.D., Murray M.A., Warmels R.H., 1987, A&A 185, 61
Smoker J.V., 1993, Ph.D. Thesis, The University of Manchester
Smoker J.V., Axon D.J., Davies R.D., 1999, A&A 341, 725
Staveley-Smith L., 1985, Ph.D. Thesis, The University of Manchester
Staveley-Smith L., Davies R.D., 1987, MNRAS 224, 953
Staveley-Smith L., Davies R.D., Kinman T.D., 1992, MNRAS 258, 334
Taylor C.L., Brinks E., Skillman E.D., 1993, AJ 105, 128
Taylor C.L., Brinks E., Pogge R.W., Skillman E.D., 1994, AJ 107, 971
Taylor C.L., Brinks E., Grashuis R.M., Skillman E.D., 1995, ApJS 99, 427
Terlevich R., Melnick J., Masegosa J., Moles M., Copetti M.V.F., 1991, A&AS 91, 285
Thuan T.X., Martin G.E., 1981, ApJ 247, 823
Thuan T.X., Lipovetsky V.A., Martin J.-M., Pustilnik S.A., 1999, A&AS 139, 1
Tyson N.D., Scalo J.M., 1988, ApJ 329, 618
van der Hulst J.M., Skillman E.D., Smith T.R., et al., 1993, AJ 106, 548
van Zee L., Haynes M.P., Giovanelli R., 1995, AJ 109, 990
Weinberg D.H., Szomoru A., Guhathakurta P., van Gorkom J.H., 1991, ApJ 372, L13
Zwicky F., 1971, Catalogue of Selected Compact Galaxies and Post-Eruptive Galaxies. Published by the author, Switzerland